Second-generation TNFα turnover model for improved analysis of test compound interventions in LPS challenge studies

European Journal of Pharmaceutical Sciences 165 (2021) 105937

Contents lists available at ScienceDirect

European Journal of Pharmaceutical Sciences

journal homepage: www.elsevier.com/locate/ejps

Second-generation TNFα turnover model for improved analysis of test compound interventions in LPS challenge studies

Julia Larsson [a,b,*], Edmund Hoppe [c,1], Michael Gautrois [c], Marija Cvijovic [b], Mats Jirstrand [a]

[a] Fraunhofer-Chalmers Centre, Chalmers Science Park, 412 88 Gothenburg, Sweden.
[b] Department of Mathematical Sciences, Chalmers University of Technology and University of Gothenburg, 412 96 Gothenburg, Sweden.
[c] Grünenthal GmbH, Aachen, Germany.

ARTICLE INFO

Keywords:
Tumor necrosis factor alpha
Lipopolysaccharides
Non-linear mixed effects
LPS challenge studies
Turnover models
Sprague-Dawley rats

ABSTRACT

This study presents a non-linear mixed effects model describing tumour necrosis factor alpha (TNFα) release after lipopolysaccharide (LPS) provocations in absence or presence of anti-inflammatory test compounds. Inter-occasion variability and the pharmacokinetics of two test compounds have been added to this second-generation model, and the goal is to produce a framework of how to model TNFα response in LPS challenge studies *in vivo* and demonstrate its general applicability regardless of occasion or type of test compound. Model improvements based on experimental data were successfully implemented and provided a robust model for TNFα response after LPS provocation, as well as reliable estimates of the median pharmacodynamic parameters. The two test compounds, Test Compound A and roflumilast, showed 81.1% and 74.9% partial reduction of TNFα response, respectively, and the potency of Test Compound A was estimated to 0.166 μmol/L. Comparing this study with previously published work reveals that our model leads to biologically reasonable output, handles complex data pooled from different studies, and highlights the importance of accurately distinguishing the stimulatory effect of LPS from the inhibitory effect of the test compound.

1. Introduction

Tumour necrosis factor alpha (TNFα) is a pro-inflammatory cytokine responsible for several immuno-responses and is involved in various signalling pathways in the body (Holbrook *et al.*, 2019). Due to its role in the pathogenesis of several immune-mediated diseases, it is considered an important biomarker for target engagement in the treatment against immune-mediated diseases, such as rheumatoid arthritis and Crohn's disease (Palladino *et al.*, 2003). Although TNFα is one of the most studied pro-inflammatory cytokines (Tisoncik *et al.*, 2012) there still exist a necessity of adding more information to the meta-analysis, for better understanding of TNFα disposition and for discrimination and ranking of test compounds in drug discovery.

A problem with studying the response of TNFα to different interventions is that circulating TNFα is often undetectable in plasma in healthy organisms. To resolve this, pro-inflammatory challengers such as lipopolysaccharides (LPS) are used to induce cell activation and release of TNFα through proteolytic cleavage of a TNFα-precursor by TNFα converting enzyme TACE (Scheller *et al.*, 2011). Exposure to LPS causes a rapid, transient and measurable release of TNFα in plasma, as well as a strong systemic inflammation response similar to that observed in sepsis (Brooks *et al.*, 2020; Pfalzgraff and Weindl, 2019; van Lier *et al.*, 2019). Although a bolus dose of LPS may not accurately represent the prolonged exposure to, mostly unknown, exogenous or endogenous factors driving the chronic inflammatory observed in patients (Medzhitov 2008), experimental administration of exogenous LPS to preclinical animals is frequently used to develop robust *in vivo* inflammation models for the identification of anti-inflammatory therapeutic drugs (Chakraborty *et al.*, 2005; Gozzi *et al.*, 1999; Shu *et al.*, 2011; Wyska, 2010; Xiang *et al.*, 2018). In addition, LPS challenge models can bridge preclinical rodent models in early drug discovery to proof-of-concept and target engagement studies in clinical trials, see for example (Kwak *et al.*, 2005; Schafer *et al.*, 2012; Seehase *et al.*, 2012; Gottlieb *et al.*, 2008). At each level in the drug development process, the LPS challenge data were critical for the definition of drug potency, efficacious concentrations and pharmacological active doses. The LPS challenge model for TNFα release was therefore key for the overall research and development strategy.

* Corresponding author
E-mail address: julia.larsson@fcc.chalmers.se (J. Larsson).
[1] Current address: Boehringer-Ingelheim GmbH & Co. KG, Drug Metabolism and Pharmacokinetics, Biberach a.d. Riss, Germany.

https://doi.org/10.1016/j.ejps.2021.105937
Received 16 April 2021; Received in revised form 31 May 2021; Accepted 4 July 2021
Available online 11 July 2021

Despite the frequent use, there are also some technical issues with LPS challenge studies. Comparison of large sets of compounds is confounded by high batch-to-batch and inter-study variability typically seen with LPS (Gozzi *et al.*, 1999; Wang *et al.*, 2007). In addition, since time-concentration data of LPS, multiple LPS dose levels, and baseline responses of TNFα are often lacking, it leads to uncertainties when distinguishing the stimulatory and inhibitory relationship between LPS provocation and test compound intervention when studying TNFα response data.

In the absence of measured LPS concentration data, the pharmacokinetic and pharmacodynamic modelling of the stimulatory effect of LPS can be described using a biophase model, which is used as a tool to understand the phenomena of LPS provocation despite the lack of information. Many of the already existing models for studying pharmacodynamic effects *in vivo* simplifies the plasma TNFα production after LPS induction with discontinuous functions, using either two zero-order inputs (Chakraborty *et al.*, 2005; Hu *et al.*, 2019) or a zero-order TNFα synthesis rate together with a time-dependent first-order release rate (Gozzi *et al.*, 1999; Shu *et al.*, 2011; Wyska, 2010). Continuous models of TNFα production after LPS induction exist as well, such as a linearly stimulated turnover model connected to a series of transit compartments (Gabrielsson *et al.*, 2015), but are not as frequently used. However, a common theme for all previous models is that the description of the stimulatory effect of LPS is kept simple, and only one dose of LPS is most commonly used throughout the study. In addition, although TNFα response data show high variability, only one of the models captures this using a non-linear mixed effects (NLME) approach (Hu *et al.*, 2019). It is thus questionable how well the stimulatory effect of LPS in TNFα response data is characterized, which in turn questions the reliability of the estimated pharmacodynamic effect since this problem has not been addressed in previous models.

The goal with this work is to produce a framework of how to model TNFα response in LPS challenge studies *in vivo* and demonstrate its general applicability regardless of occasion or type of test compound. With this framework we want to: 1) accurately distinguish the stimulatory effect of LPS from the inhibitory effect of the test compound, to get robust and reliable estimates of the pharmacodynamic parameters, 2) introduce a model structure that considers inter-occasion variability and allows for testing of multiple test compounds, and 3) fill the existing knowledge gaps concerning LPS challenge models from a biological perspective. To achieve this, we improved a previously published model by our group (Held *et al.*, 2019), demonstrated the improved model's general applicability, and validated the results by comparing them with previously published data. This second-generation model has been developed using TNFα response data consisting of multiple LPS challenge doses from different studies, as well as data from two different test compounds. The simultaneous exploration of all available animal data to the maximum extent is in the spirit of the *Three Rs* (3Rs; Replacement, Reduction, and Refinement) as the guiding principle for more ethical use of animals in research testing (Russell and Burch, 1959). Lastly, NLME modelling has been used to capture the vast variability typically seen in TNFα response data.

2. Materials and Methods

The study presented here reuses data originally published by Held *et al.* (2019) and the additional data used in this work have been retrieved using the same methodology. The model derived in the course of his work, named second-generation model, focuses on the general fit to multiple data sets and represents the natural extension of our previously published, first-generation model which captures specific trends in a limited data set. Therefore, the following sections present the description of the materials and methods developed for this specific study, while only an abbreviate summary is provided for our previously published data and first-generation model (for in-depth knowledge, see Held *et al.* (2019)).

2.1. Chemicals

Lipopolysaccharides (LPS) from *Escherichia coli* 0111:B4 was obtained from Sigma (Product number L4391) where the same batch, 036M4070V, was used in all four studies. The two test compounds are Test Compound A and roflumilast, where Test Compound A was synthesized at Grünenthal, Aachen, Germany (batch purity of $> 95\%$) while Roflumilast was supplied by Dart NeuroScience. Roflumilast is an already established active substance used for treatment against COPD and asthma (Li *et al.*, 2018), and is rapidly metabolised by cytochrome P450 isoenzymes 3A4 and 1A2 to its active metabolite roflumilast N-oxide (Lipari *et al.* 2013). Test Compound A, roflumilast, and roflumilast N-oxide are all selective inhibitors of phosphodiesterase 4 (PDE4). However, roflumilast and roflumilast N-oxide do not discriminate between the different PDE4 subtypes (Hatzelmann *et al.*, 2010), while Test Compound A is more selective for the PDE4B subtype. Inhibition of PDE4 leads to accumulation of intracellular levels of cAMP, that in turn affects the regulation of pro- and anti-inflammatory synthesis of cytokines, and has been shown to reduce LPS induced TNFα release (Li *et al.*, 2018). For a summary of the different physico-chemical properties of Test Compound A and roflumilast, see Table 1.

2.2. Animals and design of in vivo studies

The experiments were conducted in a total of 78 male Sprague-Dawley rats (210-260 g of body weight), all purchased from Vital River Laboratory Animals Co. LTD. All rats were housed in groups under 12 h light/dark cycle with *ad libitum* access to food and water. During the study, animals were not fasted, but no food was provided prior to dosing until 3 h after drug dosing. The animals were handled in strict accordance with the Guide for the Care and Use of Laboratory Animals in an AAALAC-accredited facility, and all animal studies were approved by an established Institutional Animal Care and Use Committee (IACUC).

The Sprague-Dawley rats were randomly divided into groups of six with increasing doses of LPS and test compound, respectively (Table 2). After visual inspection of the raw data, one animal from Study 2 was excluded due to an obvious deviating behaviour from the population, see Fig. S.1 and S.2 in Supplementary material. To retrieve the doses of LPS, Test Compound A and roflumilast, respectively, starting with LPS, it was dissolved in saline at 0, 0.0002, 0.0006, 0.002, 0.006 and 0.06 mg/mL and the solutions of 5 mL/kg were injected via foot dorsal vein, to give intravenous doses of 0, 1, 3, 10, 30, and 300 μg/kg, respectively. Secondly, Test Compound A was suspended in 1% HPMC (5 mPa s, Colorcon) and 0.5% Tween 80 (Sigma) in water at concentrations of 0, 0.06, 0.6, and 6 mg/mL and administered orally at a volume of 5 mg/mL, resulting in doses of 0, 0.3, 3, and 30 mg/kg, respectively. Lastly, roflumilast was dissolved in 1% HPMC and 0.5% Tween 80 in water at concentrations of 0 and 2 mg/mL and administered orally at a volume of 5 mg/mL, resulting in doses of 0 and 10 mg/kg. All animals were given either an intravenous dose of LPS or vehicle (saline), as well as either an oral dose of test compound or vehicle (1% HPMC and 0.5% Tween 80 in water).

The experimental design of the four studies is further visualised

Table 1
Physico-chemical properties of Test Compound A and roflumilast

Parameter	Value, Test Compound A	Value, roflumilast National Center for Biotechnology Information, 2021
Molecular weight	< 500 g/mol	403.2 g/mol
LogP*	< 2.5	4.6
Polar surface area	< 80 Å^2	60.4 Å^2
Solubility	10 μmol/L at pH 7.4	Insoluble (1.29 – 1.39 μmol/L at 22°C)

* cLogP for Test Compound A and XLogP3-AA for roflumilast

Table 2
Overview of experimental design of the four studies

Study	Challenge compound	Test compound	Biomarker	Designs
1.1	LPS	-	TNFα	Three challenge doses (3, 30 and 300 μg/kg) and one vehicle group (0 μg/kg); lacks challenger time course (s); no test compound intervention
1.2	LPS	-	TNFα	Four challenge doses (1, 3, 10 and 30 μg/kg) and one vehicle group (0 μg/kg); lacks challenger time course (s); no test compound intervention
2	LPS	A	TNFα	One LPS challenge dose (30 μg/kg); lacks challenger time course(s); three test compound intervention doses (0.3, 3 and 30 mg/kg)
3	LPS	roflumilast	TNFα	Three LPS challenge doses (3, 30 and 300 μg/kg); lacks challenger time course(s); one test compound intervention dose (10 mg/kg)

(Fig. 1). The challenge experiments in Study 1.1 and 1.2 (Fig. 1A and B) were conducted to characterise the dose-response-time relationships of the TNFα release after LPS challenge. In addition, they served as vehicle groups for Study 3 and 2 (Fig. 1D and C), respectively, as the experiments in Study 1.1 and 3 were conducted on one occasion and Study 1.2 and 2 on a different occasion, both as parts of one large drug discovery program. To consider the effect of inter-occasion variability, the same doses of LPS were used in both studies (3 and 30 μg/kg), which enabled a quantification of the difference in TNFα response between the occasions. The Test Compound A intervention (Fig. 1C) was conducted to characterise the inhibiting effect of the test compound for different doses. On the contrary, the roflumilast intervention was conducted as a positive control where strong inhibition is intended for the given oral dose, and is used to assess test validity (Fig. 1D).

Test Compound A, roflumilast, and roflumilast N-oxide concentrations, as well as TNFα response, were measured and analysed by mathematical modelling. On the contrary, LPS exposure could not be measured but was instead represented using a biophase model in the mathematical framework. The test compounds were administered two hours before the LPS challenge, and blood samples were drawn for quantification of Test Compound A, roflumilast, roflumilast N-oxide and TNFα at 0 h (prior to dosing of test compound), at 1 and 2 h (prior to dosing of LPS) and at 2.5, 3, 3.5, 4, 5, and 6 h after LPS dosing.

2.3. Bioanalytical methods

TNFα concentrations in plasma were quantified using the rat TNFα Quantikine ELISA Kit (R&D Systems, SRTA00), while the test compound concentrations were quantified using LC-MS/MS analysis. The lower limit of quantification (LLOQ) was 12.5 ng/L for TNFα, 1 nM for Test Compound A and roflumilast N-oxide, and 0.1 nM for roflumilast. Lower values were reported as "LLOQ" and excluded from subsequent evaluation and parameter estimation. For in-depth information concerning the bioanalytical methods, see Held *et al.* (2019).

2.4. Pharmacokinetic and pharmacodynamic models

2.4.1. Exposure to Test compounds A, roflumilast and roflumilast N-oxide

Test Compound A is modelled as a first-order loss from the gut into plasma, and the plasma exposure is given by first-order input and Michaelis-Menten elimination (Fig. 2A.1, Eq. (1) and (2)

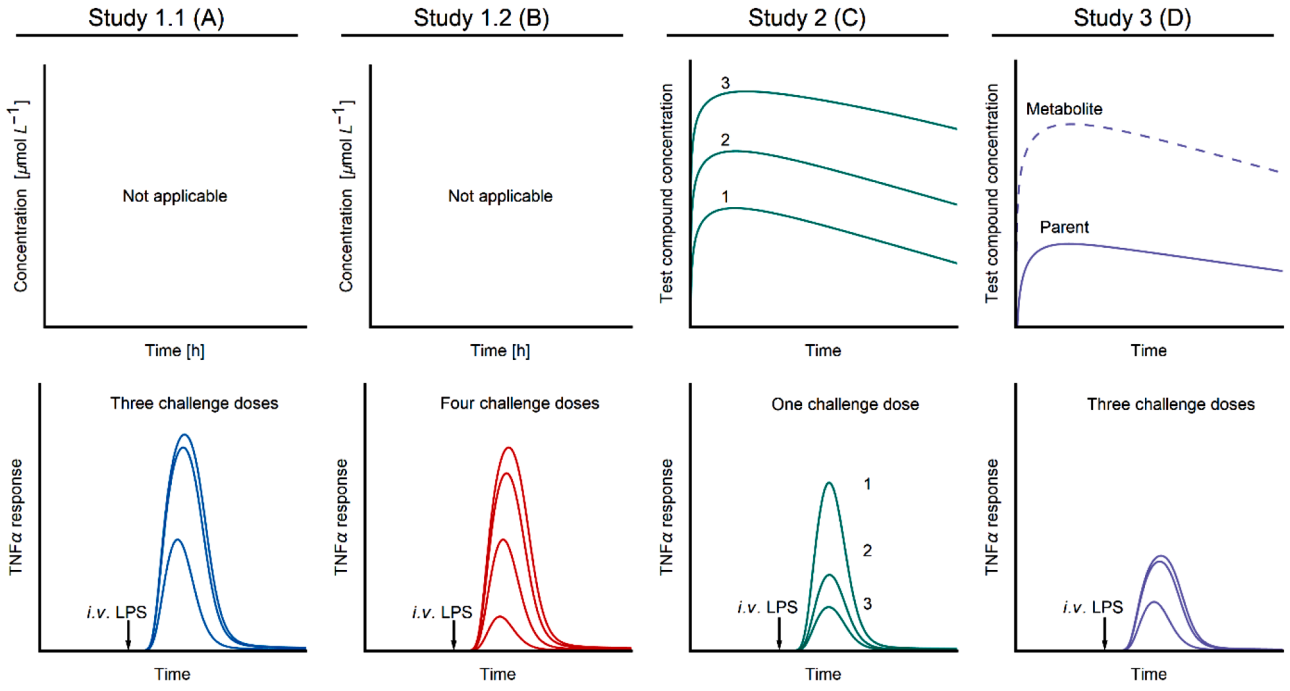

Fig. 1. Schematic presentation of the four different study designs. (A, B) Description of the challenge experiments where three (3, 30, 300 μg/kg LPS) and four (1, 3, 10, 30 μg/kg LPS) challenge doses were used, respectively. Vehicle controls were made for both studies (0 μg/kg LPS, not shown), and overlapping LPS doses between the studies (3, 30 μg/kg LPS) enabled quantification of inter-occasion variability. Study 1.1 and 1.2 served as test compound vehicle controls for Study 3 and 2, respectively. (C) Description of the test compound intervention using Test Compound A. Three oral doses were used (0.3, 3, 30. mg/kg Test Compound A) for a constant challenge dose (30 μg/kg LPS) and concentration-time data for Test Compound A is available. (D) Description of the positive control using roflumilast. One constant oral dose was used (10 mg/kg roflumilast) for varying challenge doses (3, 30 and 300 μg/kg LPS) and concentration-time data for roflumilast parent drug and its active metabolite roflumilast N-oxide are available.

$$\frac{dA_{ab}}{dt} = -k_a A_{ab} \quad (1)$$

$$V_p \cdot \frac{dC_p}{dt} = F \cdot k_a \cdot A_{ab} - \frac{V_{max} \cdot C_p}{K_m + C_p} \quad (2)$$

where A_{ab} and C_p denote amount in the gut and plasma concentration of Test Compound A, respectively. The parameter k_a is the first-order absorption rate constant, V_p is the volume of distribution, V_{max} is the maximum rate of elimination, and K_m is the Michaelis-Menten constant. Michaelis-Menten elimination was chosen since the exposure to test compound increased disproportionately with increasing doses (see Fig. S.1 in Supplementary material). F denotes the bioavailability and is set to unity due to lack of intravenous data (effectively this means that estimates of V_p potentially includes effects of non-unity bioavailability). The pharmacokinetic model for Test Compound A serves to drive the pharmacodynamics to get accurate estimates of I_{max} and IC_{50} from the TNFα response data.

For roflumilast and its active metabolite roflumilast N-oxide, a simple analytic equation for first-order extravascular input and output is used in both cases (Fig. 2A.2, Eq. (3) and (4))

$$C_r(t) = A\left(e^{-k_{a,r}t} - e^{-k_{e,r}t}\right) \quad (3)$$

$$C_m(t) = B\left(e^{-k_{a,m}t} - e^{-k_{e,m}t}\right) \quad (4)$$

where C_r and C_m denote roflumilast and roflumilast N-oxide exposure in plasma, respectively. The parameters A and B are concentration constants, $k_{a,r}$ is the first-order absorption rate constant, $k_{a,m}$ is the metabolite formation rate constant, and $k_{e,r}$ and $k_{e,m}$ are the elimination rate constants, respectively. All simplifications are due to the study design of the positive control and the models are used to verify that the pharmacokinetics of roflumilast are independent of LPS dose (Table 2). For a more elaborate derivation of the pharmacokinetic models of roflumilast and roflumilast N-oxide, see Supplementary material.

2.4.2. Turnover of TNFα response after LPS challenge

The stimulatory effect on TNFα response by LPS is described in Fig. 2C and Eq. (5) and (6). A one-compartment disposition model of the LPS mixture with parallel first- and second-order loss of LPS is inferred from TNFα response-time data from the challenge experiments

$$\frac{dA_{LPS}}{dt} = -k_{LPS,1}A_{LPS} - k_{LPS,2}A_{LPS}^2 \quad (5)$$

where A_{LPS} denote LPS amount in the biophase, and $k_{LPS,1}$ and $k_{LPS,2}$ are the first-order and second-order elimination constants of LPS, respectively.

The level of LPS in plasma triggers an intra-cellular signalling cascade leading to TNFα release, which is modelled by a series of transduction compartments triggered by a bounded signal, modelled as a saturable function of the level of LPS

$$\begin{aligned} \frac{dS_1}{dt} &= -k_s \cdot \left(\frac{A_{LPS}}{K_{m,LPS} + A_{LPS}} - S_1\right) \\ \frac{dS_2}{dt} &= -k_s \cdot (S_1 - S_2) \\ \frac{dS_3}{dt} &= -k_s \cdot (S_2 - S_3) \end{aligned} \quad (6)$$

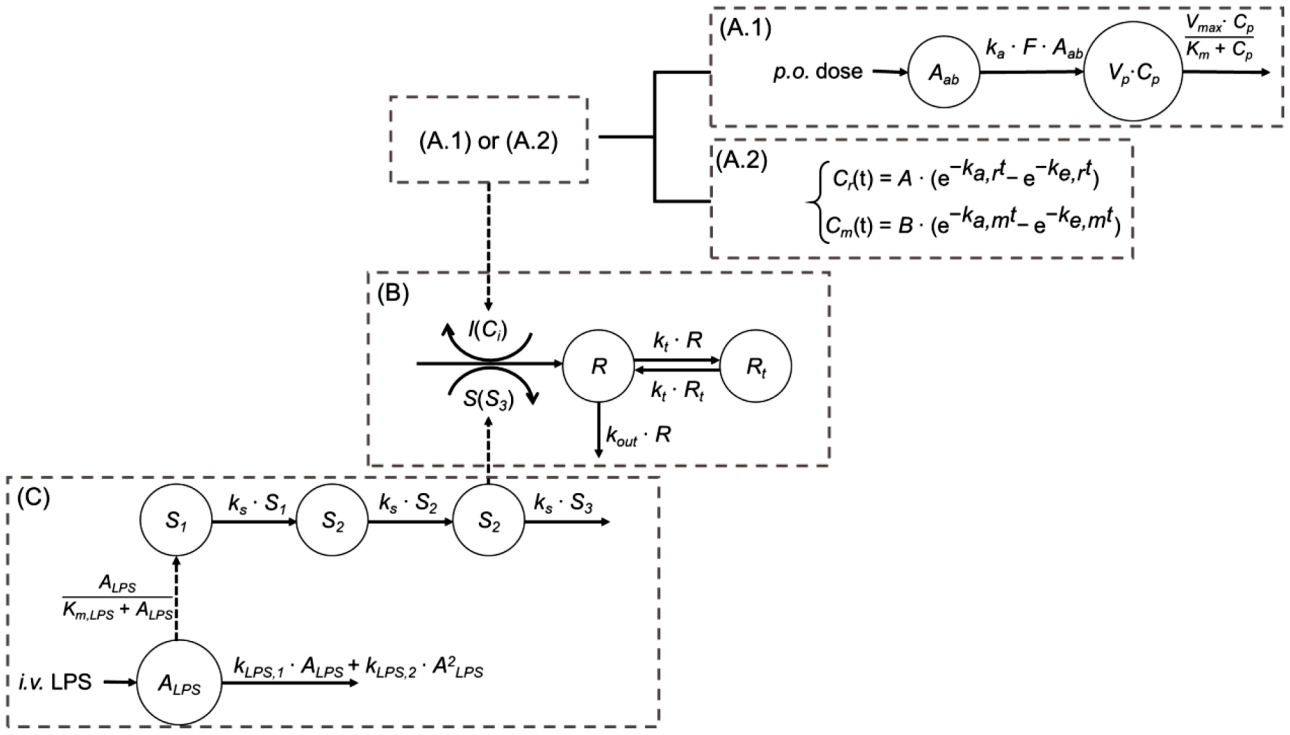

Fig. 2. Schematic presentation of the pharmacokinetic and pharmacodynamic model. Solid arrows represent mass transfer and dashed arrows stand for controls (information flow). (A.1) Pharmacokinetic model of Test Compound A disposition after oral administration. Test Compound A undergoes linear absorption from gut to plasma and is eliminated from plasma through Michaelis Menten elimination. (A.2) Pharmacokinetic model of test compound disposition after oral administration for roflumilast and its active metabolite roflumilast N-oxide. The pharmacokinetics of roflumilast and roflumilast N-oxide are modelled independently using the analytic equation for first-order extravascular input and output. (B) Turnover model for the TNFα response. TNFα is divided into pools R and R_t. Here, k_t and k_{out} denote the first-order transfer constant between compartments and fractional turnover rate constant from the system, respectively. TNFα turnover is stimulated by LPS challenge from part C and inhibited by test compound pharmacokinetics from part A.1 or A.2. (C) Model of LPS challenge. A biophase A_{LPS} describes LPS after intravenous administration with a mix of first-order and second-order elimination kinetics governed by $k_{LPS,1}$ and $k_{LPS,2}$. LPS non-linearly stimulates a signal chain (S_1 to S_3) with half-maximal signal constant $K_{m,LPS}$, and signal transduction constant k_s.

where S_1, S_2, and S_3 are unitless signalling entities and S_3 acts on the build-up of TNFα response via stimulatory action. The parameter $K_{m,LPS}$ is a half-maximal signal constant and k_s is a transduction constant inversely proportional to the delay time induced by the transduction compartments (Savic *et al.*, 2007). LPS is assumed to be eliminated through a mix of first-order and second-order kinetics as the exploratory data analysis indicated that LPS elimination increased for increasing LPS doses.

2.4.3. Turnover of TNFα response after LPS and test compounds

The TNFα turnover R and the impact of both the LPS challenge and the test compound kinetics on the TNFα response is described in Fig. 2B and Eq. (7)-(10). The stimulatory action of LPS $S(S_3)$ on the TNFα release is described using a sigmoidal function

$$S(S_3) = \frac{S_{max} \cdot S_3^{\gamma}}{SC_{50}^{\gamma} + S_3^{\gamma}} \tag{7}$$

where S_{max} is the maximum LPS stimulatory production rate of TNFα, SC_{50} is the concentration of S_3 at 50% maximum stimulation, and γ the Hill coefficient.

The inhibitory action $I(C_p)$ of Test Compound A is described using an ordinary inhibitory I_{max} model

$$I(C_p) = 1 - \frac{I_{max} \cdot C_p}{IC_{50} + C_p} \tag{8}$$

where I_{max} is the maximum inhibitory effect (test compound efficacy) and IC_{50} the drug concentration resulting in 50% maximum inhibitory effect (test compound potency).

The inhibitory action $I(C_r + C_m)$ of roflumilast and roflumilast N-oxide is described using an ordinary inhibitory I_{max} model, which is assumed to operate in saturation during the course of the experiment (roflumilast and roflumilast N-oxide is assumed to be persistently higher than IC_{50}):

$$\begin{aligned} &I(C_r + C_m) = 1 - \frac{I_{max} \cdot (C_r + C_m)}{IC_{50} + (C_r + C_m)} \approx 1 - I_{max}, \\ &C_r + C_m \gg IC_{50} \end{aligned} \tag{9}$$

The simplified inhibitory action of roflumilast is required due to the study design of the positive control (Table 2), and the inhibiting properties of roflumilast and roflumilast N-oxide are assumed to be similar (Hatzelmann *et al.*, 2010). Eq. (7) and (8) or (9) will then enter Eq. (10), where TNFα release is either stimulated or simultaneously stimulated and inhibited:

$$\begin{aligned} \frac{dR}{dt} &= S(S_3) \cdot I(C_i) - k_{out} \cdot R + k_t \cdot (R_t - R) \\ \frac{dR_t}{dt} &= k_t \cdot (R - R_t) \end{aligned} \tag{10}$$

The dynamics of TNFα response is divided into a central pool R and a peripheral pool R_t governed by a first-order inter-compartmental rate constant k_t, in order to capture the post-peak bi-phasic decline of the response. The irreversible loss of TNFα effect occurs from its central pool with fractional turnover rate constant k_{out}. Due to the lack of TNFα baseline response, the zero-order constant for production of response, usually denoted k_{in}, is replaced in this turnover model with the stimulatory action of LPS $S(S_3)$, to ensure that the TNFα response is only non-zero in presence of LPS. The inhibiting mechanism described in Eq. (10) is assumed to be similar for all compounds, since Test Compound A, roflumilast, and roflumilast N-oxide are all selective inhibitors of PDE4.

2.4.4. Data analysis

To add the inter-individual variability, an NLME approach is used (Lindstrom and Bates, 1990). Inter-individual variability is given to the parameters that either have the largest impact on the model output or are of special interest from a model predictive perspective. Therefore, distributions are assigned to the following parameters: V_{max} (Eq. (2)) normally distributed, $k_{e,r}$, $k_{e,m}$, $k_{LPS,1}$, IC_{50} (Eq. (3)-(5), and (8)) log-normally distributed, and I_{max} (Eq. (9)) logit-normally distributed.

To accurately distinguish the stimulatory effect of LPS from the inhibitory effect of the test compounds, parameter estimation is done sequentially. Firstly, the pharmacokinetic parameters of Test Compound A, roflumilast, and roflumilast N-oxide (k_a, V_p, V_{max}, K_m, Eq. (1)-(2), and A, B, $k_{a,r}$, $k_{a,m}$, $k_{e,r}$, $k_{e,m}$, (Eq. (3)-(4)) are estimated using time-concentration data of the test compounds (Fig. 1C and D). Secondly, the parameters governing TNFα response after LPS provocation ($k_{LPS,1}$, $k_{LPS,2}$, $K_{m,LPS}$, k_s, S_{max}, SC_{50}, γ, k_{out}, k_t, Eq. (5)-(7) and (10)) are estimated using data from Study 1.1 and 1.2 (Fig. 1A and B). Lastly, the parameters describing test compound potency and efficacy (I_{max}, IC_{50}, Eq. (8)-(9)) are estimated using TNFα response data from Study 2 or 3 (Fig. 1C and D). In the last step, all other parameters are fixed to their previously estimated values, and the inter-individual variability for $k_{LPS,1}$ is removed since it was shown to interfere (due to non-identifiability) with the estimation of the median pharmacodynamic parameters.

The studies were conducted at two different occasions as parts of one large drug discovery program, and since a notable difference in TNFα response was observed between the two occasions an inter-occasion variability is implemented. The chosen approach is based on Laporte-Simitsidis *et al.* (2000): The parameter with the largest impact on the discrepancy between the studies is estimated according to Eq. (11)

$$\begin{aligned} k_{LPS,2} &= k_{LPS} + \delta \cdot I_{occasion}, \\ I_{occasion} &= \begin{cases} 1, \text{if individual belong to Study 1.2 or 2} \\ 0, \text{if individual belong to Study 1.1 or 3} \end{cases} \end{aligned} \tag{11}$$

where k_{LPS} and δ are estimated using TNFα response data from Study 1.1 and 1.2 (Fig. 1A and B), and used when estimating the pharmacodynamic effect of Test Compound A from Study 2 (Fig. 1C) and roflumilast from Study 3 (Fig. 1D), respectively.

The observation error for the Test Compound A measurements is modelled with an additive error model on log-scale, and for the roflumilast and roflumilast N-oxide measurements a proportional error model is used. The observation error for the TNFα response concentrations is modelled with a proportional error model as well. These choices of error models are based on the wide ranges of both test compound and TNFα response concentrations, as well as on a systematic model evaluation using different error models. All modelling and parameter estimation is done using Wolfram Mathematica 12 and *NLMEModeling* – an NLME modelling package developed by Fraunhofer-Chalmers Centre (Leander *et al.* 2020).

3. Results

3.1. Experimental data and explorative data analysis

Our second-generation model (Fig. 2) captures the inter-individual variability, inter-occasion variability, and the general trends observed in data (Fig. 3, notice the twice as large concentration range for Study 1.1). Although the number of Sprague-Dawley rats in each group is relatively small, a large variety in especially TNFα response is observed, supporting the use of the NLME modelling framework. Detailed information of each data diagram can be found in the Supplementary material.

The area under TNFα response curves ($AUC_{TNFα}$) were used to assess the net effect of LPS provocation or test compound treatment from an exploratory data analysis perspective, which is commonly done for TNFα response in LPS challenge studies (Chakraborty *et al.*, 2005; Gozzi *et al.*, 1999; Held *et al.*, 2019; Hu *et al.*, 2019; Wang *et al.*, 2007). The $AUC_{TNFα}$ were calculated for all individuals in Fig. 3 (bottom row) and are summarised in boxplots (Fig. 4). In addition, a Mann-Whitney U test

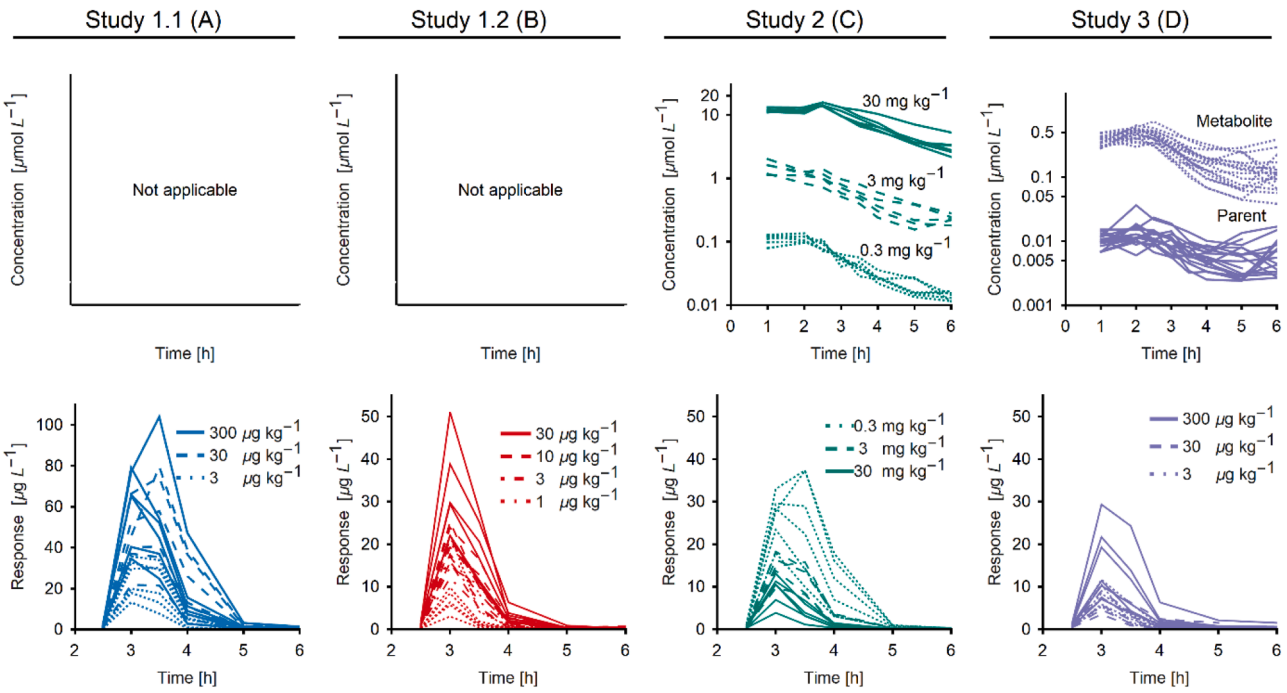

Fig. 3. Summary of the available data from the four different studies (notice the twice as large concentration range for Study 1.1). (A, B) TNFα response data after three (3, 30, 300 μg/kg LPS) and four (1, 3, 10, 30 μg/kg LPS) challenge doses, respectively (no test compound dosing). (C) TNFα response and time-concentration data of Test Compound A. Three oral doses were used (0.3, 3, 30. mg/kg Test Compound A) for a constant challenge dose (30 μg/kg LPS). (D) TNFα response and time-concentration data of roflumilast. One constant oral dose was used (10 mg/kg roflumilast) for varying challenge doses (3, 30 and 300 μg/kg LPS). For more information concerning the study design, see section 2.2.

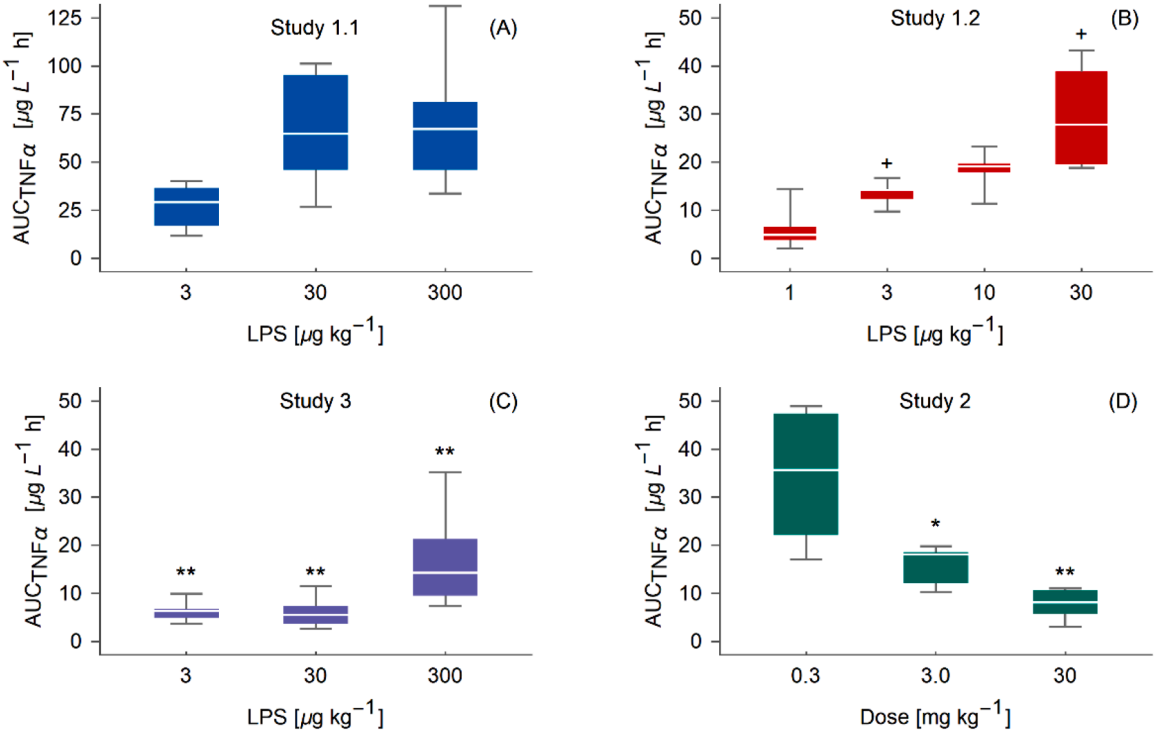

Fig. 4. Area under the TNFα response curves ($AUC_{TNF\alpha}$), summarised in boxplots for each dose group, versus either increasing LPS challenge doses or oral doses of test compound for the different studies. (A) Increasing LPS challenge doses (3, 30 and 300 μg/kg LPS, Study 1.1). (B) Increasing LPS challenge doses (1, 3, 10 and 30 μg/kg LPS, Study 1.2) where the common LPS doses with Study 1.1 are significantly different from each other (p-value < 0.05). (C) Constant oral dose of test compound (10 mg/kg, roflumilast) and increasing LPS challenge doses (3, 30 and 300 μg/kg, Study 3), all significantly different from the corresponding controls in Study 1.1 (p-value < 0.01). (D) Increasing oral doses of test compound (0.3, 3 and 30 mg/kg, Test Compound A) and a fixed LPS challenge dose (30 μg/kg, Study 2), either not significant, significant, or very significant relative control (30 μg/kg LPS dose Study 1.2, p-value < 0.05 or < 0.01, respectively).

was performed to investigate significant difference between drug intervention and control as well as significant difference in response between occasions for common LPS doses (see Table 2) (van Eijk *et al.*, 2014). Significance is denoted with a * or + (p-value < 0.05) and ** (p-value < 0.01), respectively. The trends between boxplots indicate a necessity of inter-occasion variability and supports the suggested stimulatory and inhibitory action of LPS and test compounds, respectively. Starting with Study 1.1 (Fig. 4A), the range in $AUC_{TNF\alpha}$ is considerably larger than the others, and there exists a saturating trend in the boxplots for LPS doses above 30 μg/kg which have been discussed previously (Held *et al.*, 2019). For Study 1.2 (Fig. 4B) the trend is linear as saturation has not been reached for LPS doses up to 30 μg/kg, and a significant difference in response between Study 1.1 and 1.2 is prominent. For Study 3 where roflumilast is present (Fig. 4C), the $AUC_{TNF\alpha}$ are much smaller compared to Study 1.1 where test compound is absent, suggesting that maximal inhibition is reached using 10 mg/kg roflumilast thus validating the positive control. Lastly, for Study 2 where Test Compound A is present (Fig. 4D, note the different horizontal axes), a non-linear trend in the $AUC_{TNF\alpha}$ for increasing test compound doses is seen, which was captured using an ordinary inhibitory I_{max} model. In summary, there exist a saturated LPS response, a significant inter-occasion variability, a maximal inhibition with roflumilast, and a non-linear saturated response by Test Compound A, properties captured by the model through Eq. (7), (8), (9), and (11), respectively.

3.2. Model regression and parameter analysis

3.2.1. Turnover of TNFα response after LPS challenge

The mathematical model for TNFα response after LPS challenge captures the response for all LPS doses independent of study. The model predictions from both Study 1.1 and 1.2 show good individual fits as well as a successful implementation of inter-occasion variability (Fig. 5). Final parameter estimates (presented in Eq. (5), (6), and (7)) are presented in Table 3, and for the model predictions for all LPS challenge doses see Fig. S.8 in Supplementary material.

3.2.2. Turnover of TNFα response after LPS and test compound exposure

The mathematical models for TNFα response after LPS and test compound exposure suggests that the lowest dose of Test Compound A has low effect on TNFα response (Fig. 6), and that the simplified model for roflumilast sufficiently represent the positive control data (Fig. 7). Starting with Test Compound A, the predicted pharmacokinetic model (Fig. 6A, C, and E) and pharmacodynamic effect (Fig. 6B, D, and F) is shown on both population and individual level (black and grey solid lines, respectively), and the estimated potency is illustrated as a horizontal red dashed line. The population prediction of the TNFα response accurately captures the median behaviour of each dose group, while the accuracy of the individual model predictions varies. The parameter estimates for the pharmacokinetic model of Test Compound A and its inhibitory effect on the TNFα response (presented in Eq. (1), (2), and (8)) can be found in Table 4 and 5.

Table 3
Final estimates of the parameters governing the turnover of TNFα response after LPS challenge and their coefficients of variation (CV), inter-individual variability (IIV), IIV CV, and half-lives.

Parameter	Units	Estimate	CV [%]	IIV [%]	IIV CV [%]	Half-life [min]
$k_{LPS,1}$	1/h	7.12	28.3	18.1	25.3	5.84
k_{LPS}	μg/kg/h	0.567	49.2	-	-	-
δ	μg/kg/h	2.02	29.0	-	-	-
$K_{m,LPS}$	μg/kg	0.147	34.9	-	-	-
k_s	1/h	3.17	7.82	-	-	13.1
S_{max}	μg/L/h	400	14.0	-	-	-
SC_{50}	-	0.320	17.9	-	-	-
γ	-	4.65	5.28	-	-	-
k_{out}	1/h	5.20	9.66	-	-	8.00
k_t	1/h	0.453	9.91	-	-	91.9

For roflumilast and its active metabolite, the predicted pharmacokinetic model verifies that the pharmacokinetics of roflumilast are independent of LPS dose (Fig. 7A, C, and E). In addition, the population prediction of the TNFα response (Fig. 7B, D and F, black solid lines) captures the median behaviour for the lowest and highest LPS dose, and the accuracy of the individual model predictions varies (Fig. 7B, D and F, grey solid lines). The parameter estimate for the pharmacodynamic model (presented in Eq. (9)) can be found in Table 5 and the estimates of the pharmacokinetic parameters can be found in Supplementary material.

3.2.3. Contribution to biological meta-analysis

To validate the findings and confirm our contribution to the meta-analysis from a biological perspective, the results are summarised and compared with previously published results. As a confirmation of the biological plausibility of the parameter estimates, a summary of estimated TNFα elimination rates from the literature has been compiled (Table 6). Compared with the fractional turnover rate constant (*i.e.*, the elimination rate from the TNFα pool) estimated in this work (half-life 8.00min, see Table 3), our estimate corresponds well to literature data and is reasonable from a biological perspective.

To further validate successful contribution to the meta-analysis of TNFα response after LPS provocation, the second-generation model developed in this study is compared with our previously published first-generation model (Fig. 8) (Held *et al.*, 2019). The second-generation model both validates previous findings concerning properties of LPS

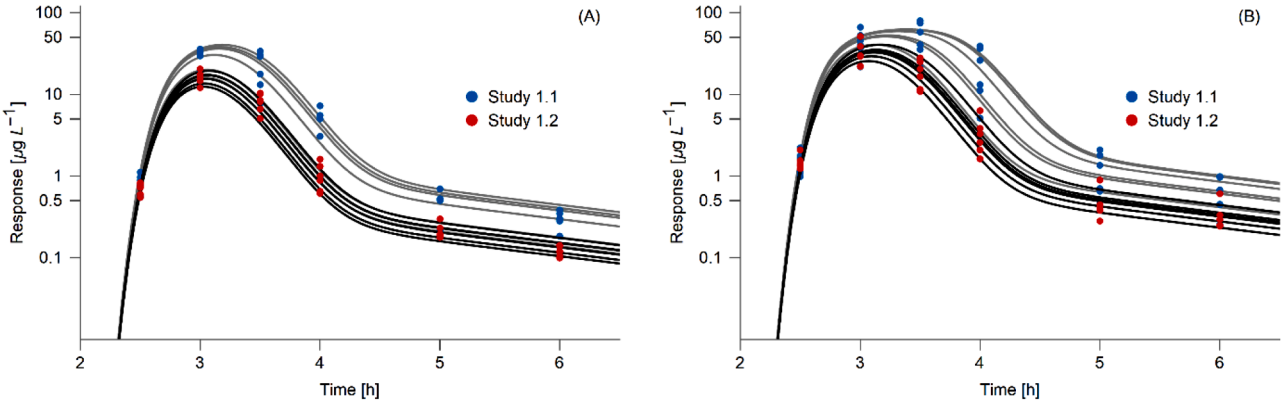

Fig. 5. Observed (dots) and model predicted (solid lines) TNFα response for both Study 1.1 (blue dots, grey lines) and 1.2 (red dots, black lines) respectively. (A) 3 μg/kg LPS. (B) 30 μg/kg LPS. For all model predicted TNFα responses from Study 1.1 and 1.2, see Fig. S.8 in Supplementary material.

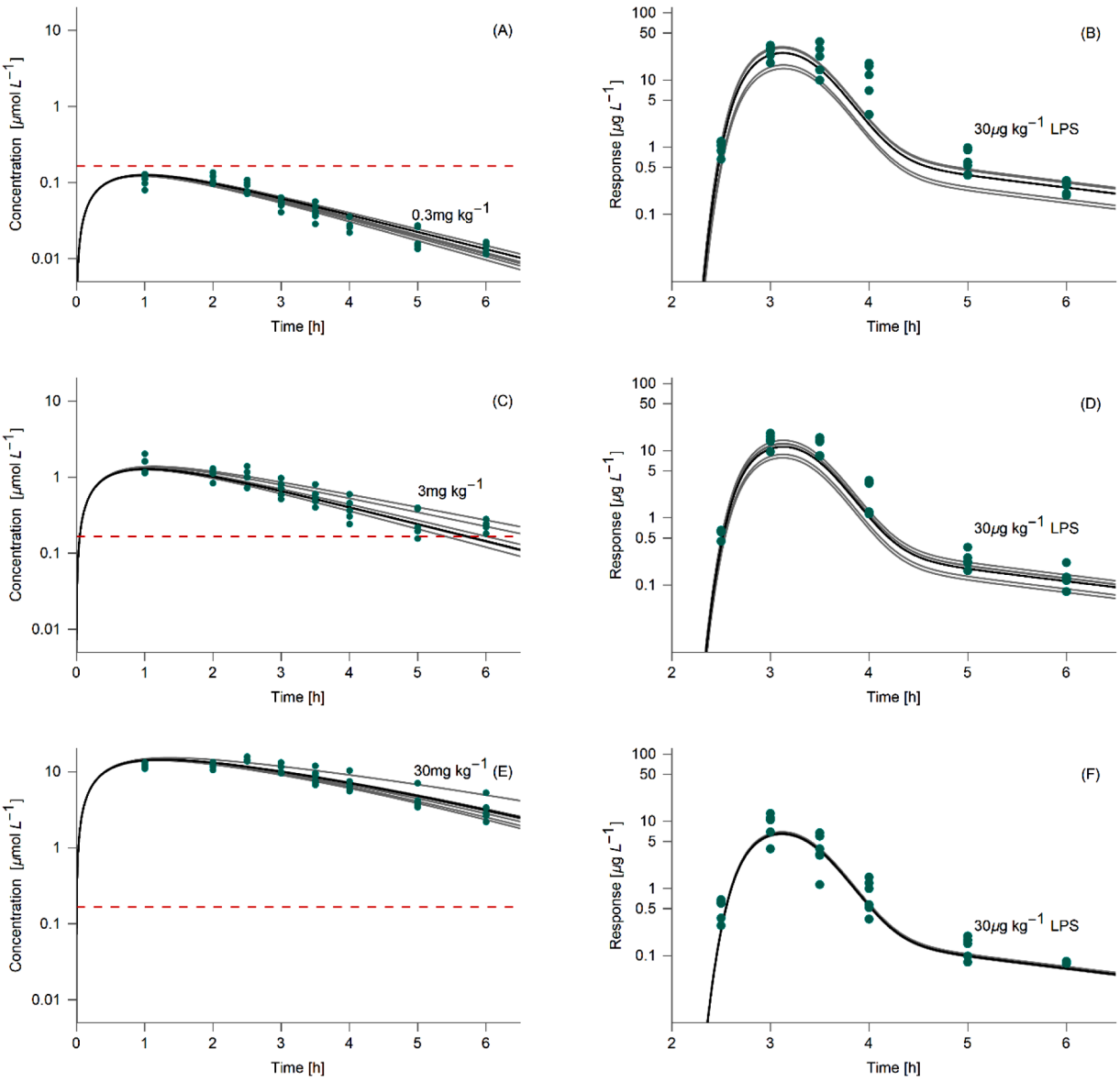

Fig. 6. (A, C, E) Observed (green dots) and model-predicted (solid lines) concentration-time data of Test Compound A of all subjects in Study 2. The grey lines correspond to the individual predictions, the black line the population prediction, and the red dashed line the model-predicted in vivo potency of Test Compound A. (B, D, F) Observed (green dots) and model-predicted (solid lines) concentration-time data of TNFα of all subjects in Study 2. The grey lines correspond to the individual predictions and the black line the population prediction. TNFα response was observed after a fixed LPS challenge of 30 μg/kg. Test compound doses were 0.3 mg/kg (panel A, B), 3 mg/kg (panel C, D), and 30 mg/kg (panel E, F). For visualisation of the control group (0 mg/kg Test Compound A, 30 μg/kg LPS), see Fig. 5B or Fig. S.8 in Supplementary material.

provocation and TNFα release as well as adds further information to the meta-analysis, thus improving the model from both a mathematical and biological perspective.

4. Discussion

In this work we developed a second-generation TNFα turnover model based on TNFα response data using multiple LPS challenge doses and two different test compounds. The model is proposed to work as a framework enabling modelling of TNFα response in LPS challenge studies *in vivo,* demonstrating a general applicability regardless of occasion, study design, or type of test compound.

4.1. Data and model analysis

The boxplots representing the $AUC_{TNF\alpha}$ showed a significant inter-occasion variability between the challenge experiments, as well as significant drug effect relative control for Test Compound A doses above 3 mg/kg, and for roflumilast for all LPS doses (Fig. 4). All mentioned trends were expected before conducting the experiments and validated through statistical testing, verifying that six animals per study was a sufficient sample size. A high inter-individual and inter-occasion variability with LPS is apparent for all studies, which was expected even though the extrinsic variability was minimized when conducting the experiments (see section 2.2). This variability is very well described in the literature and is known to cause major problems when running experiments over long periods, as is often the case in large drug discovery programs (Gozzi *et al.*, 1999; Wang *et al.*, 2007). However, although a large variation was expected the source of variation remains unknown. Most probably it's caused by poorly defined LPS, latent infections of animals, and/or differences in biological responsiveness of animals, since LPS are heterogeneous components of the cell wall of

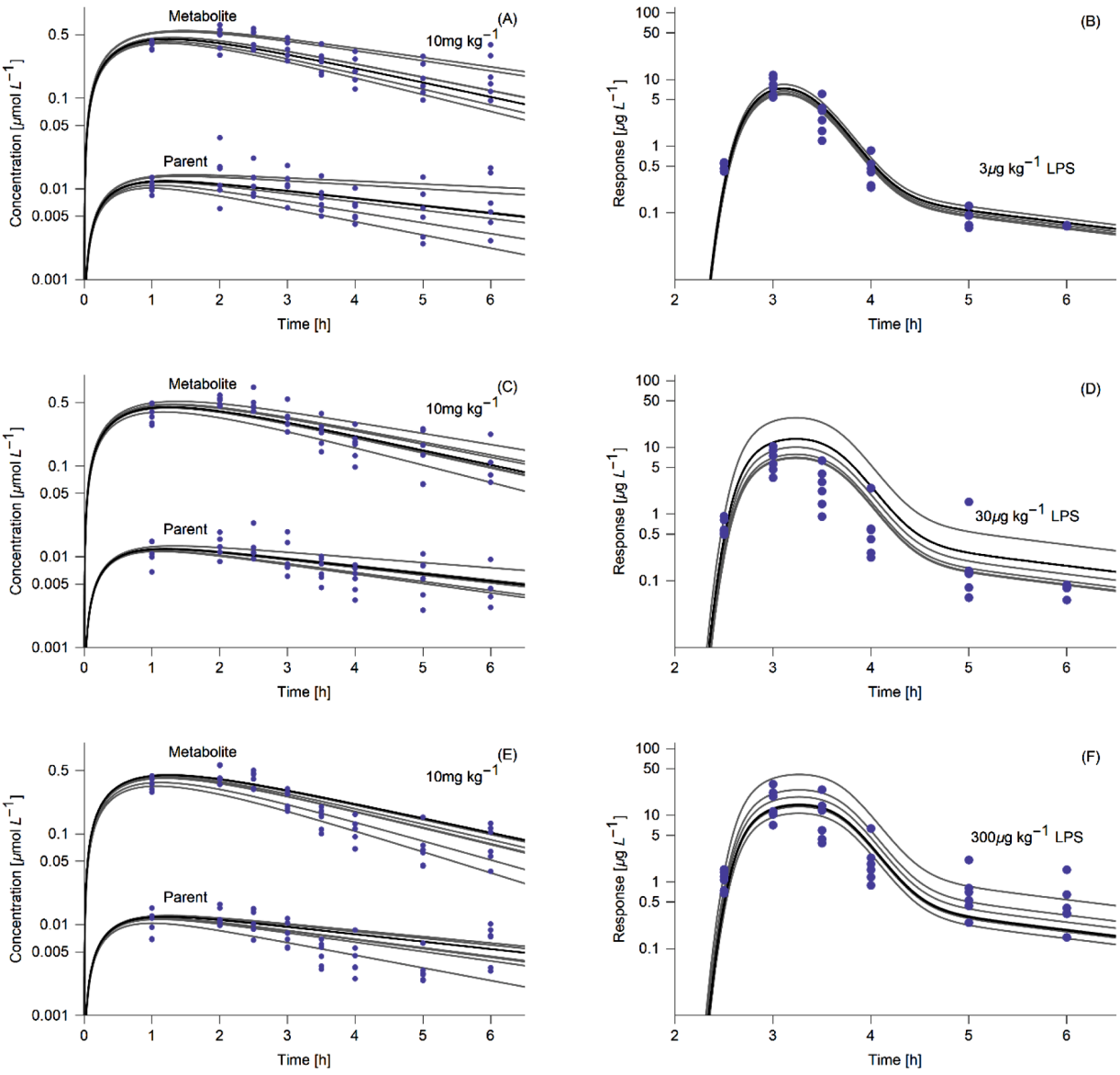

Fig. 7. (A, C, E) Observed (purple dots) and model-predicted (solid lines) concentration-time data of roflumilast and the active metabolite of all subjects in Study 3. The grey lines correspond to the individual predictions, the black line the population prediction. (B, D, F) Observed (purple dots) and model-predicted (solid lines) concentration-time data of TNFα of all subjects in Study 3. The grey lines correspond to the individual predictions and the black line the population prediction. TNFα response was observed after varying LPS challenges of 3 μg/kg (panel A, B), 30 μg/kg (panel C, D) and 300 μg/kg (panel E, F). Test compound dose were 10 mg/kg. For visualisation of the control groups (0 mg/kg roflumilast, 3, 30, 300 μg/kg LPS), see Fig. S.8 in Supplementary material.

Table 4
Final estimates of the pharmacokinetic parameters of Test Compound A and their coefficient of variation (CV), inter-individual variability (IIV), and IIV CV.

Parameter	Units	Estimate	CV [%]	IIV [%]	IIV CV [%]
k_a	1/h	1.72	12.1	-	-
V_p	L/kg	3.40	3.99	-	-
V_{max}	μmol/h/kg	32.1	16.7	11.3	52.4
K_m	μmol/L	18.1	19.2	-	-

Table 5
Final estimates of the potency and efficacy of Test Compound A, and efficacy of roflumilast and roflumilast N-oxide, together with their coefficient of variation (CV), inter-individual variability (IIV), and IIV CV.

Parameter	Units	Estimate	CV [%]	IIV [%]	IIV CV [%]
I_{max}	-	0.811	3.46	-	-
IC_{50}	μmol/L	0.166	28.2	308	71.3
I_{max}	-	0.749	19.7	21.0	46.8

Gram-negative bacteria that cannot be quantified by standard bioanalytical methods such as LC-MS/MS (Hurley 1995; Rojo *et al.*, 2007). Therefore, in the absence of a possibility for a bioanalytical LPS quantification, the LPS provocation was chosen to be described using a biophase model with inter-individual variability on the LPS elimination, which is the common approach when studying LPS challenge studies through modelling (Chakraborty *et al.*, 2005; Hu *et al.*, 2019; Gozzi *et al.*, 1999; Shu *et al.*, 2011; Wyska, 2010; Gabrielsson *et al.*, 2015).

The non-linear decreasing trend with respect to increased dose of Test Compound A suggests an ordinary inhibitory I_{max} model (Eq. (8)), which has been shown to represent data well (Fig. 6B, D and F). In addition, comparing Study 1.2 and 2 (Fig. 4B, rightmost boxplot, and 4D, leftmost boxplot) the lowest oral dose of Test Compound A has no significant effect on reducing TNFα response. This has also been

Table 6
TNFα elimination rate estimates from literature, both for different test subjects as well as from both *in vivo* and *in vitro* studies.

Species	Estimate [1/h]	CV [%]	$t_{1/2}$ [min]	Source
Mouse (*in vivo*)	-	-	6*	Beutler *et al.*, 1985
	-	-	18.6*	Dai et al., 2013
	-	16.7	12*	Shibata *et al.*, 2004
	-	23	34*	Ma *et al.*, 2015
	-	17.85	2.8*	Tsutsumi *et al.*, 1996
	0.504	21	82.5	Gozzi *et al.*, 1999
	1.65	24.4	25.2	Wyska, 2010
	4.51	-	9.22	Chakraborty *et al.*, 2005
Rat (*in vivo*)	5.65	30	7.36	Held *et al.*, 2019
Human (*in vivo*)	-	-	11-17	Moritz *et al.*, 1989
	-	-	15-30	Saks and Rosenblum, 1992
	1.82	6.48	22.8	Shu *et al.*, 2011
Mouse (*in vitro*)	0.0463	32	898	Xiang *et al.*, 2018

* Only half-life reported

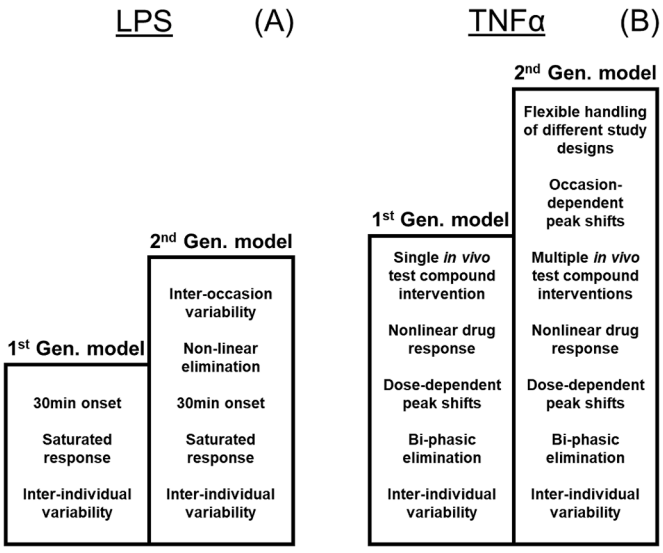

Fig. 8. Schematic illustration of model improvement between the different turnover model generations for both LPS (A) and TNFα (B).

captured by the model, as the estimated potency is larger than the maximal test compound concentration (IC_{50} = 0.166 μmol/L, Fig. 6A and Table 5). For the positive control using roflumilast, the inhibition was effectively operating at its maximal effect for the complete duration of the experiment. This is validated statistically comparing the $AUC_{TNFα}$ from Study 1.1 and 3 (Fig. 4A and C), and captured in the model using a reduced inhibitory I_{max} model (Eq. (9)). However, Eq. (9) does not explain the displacement of the $AUC_{TNFα}$ for the medium LPS dose (Fig. 4C). Our model assumes that the test compounds inhibit the maximum stimulatory effect of LPS by a factor $(1 + I_{max})$ (see Eq. (10)), but Fig. 4D indicates that roflumilast affects the apparent affinity of LPS stimulation as well. The consequence of not capturing the apparent effect on affinity is seen in Fig. 7D, where a systematic overprediction of response is visible. It could be due to intrinsic variation in biological response as described above, but that hypothesis does not support the systematic lower response. A second hypothesis therefore is that the interplay between stimulation and inhibition of TNFα response is more complex than currently described, see for example Earp *et al.* (2004). However, since this is only seen in a small fraction of the whole data set it is difficult to draw any conclusions, but it would be interesting to investigate this complex interplay in future studies. For further information concerning the model selection process based on data analysis, see Supplementary material and Held *et al.* (2019).

The exploratory data analysis presented in Fig. 4 has supported the model selection process which has led to successful fit to data and reliable parameter estimates (Fig. 5, 6, and 7). The stimulatory effect of LPS in TNFα response data is well characterized independent of study (Fig. 5, Table 3, and Fig. S.7 in Supplementary material) and the pharmacokinetics of Test Compound A is well estimated (Fig. 6A, C and E, and Table 4), both on population and individual level. The largest uncertainties in parameter estimates for these models concern the parameters governing the LPS provocation or the inter-individual variability (Table 3 and 4). This is expected as measurements of LPS concentrations are lacking and the pharmacokinetics are studied under a relative short time period (Fig. 3). For roflumilast and roflumilast N-oxide, on the other hand, improvements to the pharmacokinetic models could be made but due to their limited purpose the models were decided to be satisfactory (Fig. 7A, C and E, and Supplementary material).

Concerning the inhibitory effect, good population estimates of pharmacodynamic parameters were retrieved after removing the source of variability from LPS stimulation during the estimation (Fig. 6B, D, and F, and Fig. 7B, D and F). The variability was removed since the stimulatory and inhibitory effects otherwise became indistinguishable, leading to questionable estimates of the pharmacodynamic parameters. The drawback with deliberately removing the known variation in LPS exposure is that the observation error becomes overestimated, in turn leading to less accurate individual predictions. This is especially prominent for the TNFα response using the largest oral dose of Test Compound A, where the test compound concentrations are well above the potency and thus gets unaffected by any variation in IC_{50} (Fig. 6F). However, although the observation error and inter-individual variability becomes less accurate using this approach (see Table 5), it has led to more robust estimates of the median pharmacodynamic effect which was one of the goals with this framework.

Using this framework, IC_{50} and I_{max} for Test Compound A are estimated to 0.166 μmol/L and 0.811, respectively, and I_{max} for roflumilast is estimated to 0.749 (Table 5). These results show that our framework can retrieve pharmacodynamic estimates from data with different study designs, allowing a comparison of inhibitory effect between new test compounds (whose pharmacodynamic effects are not yet established) and positive controls. On top of that, by constructing a framework using NLME modelling and allowing pooling of data from different studies, including the positive control, the experimental data in this work have been used to its fully potential. The approach described in this manuscript has maximized the information with fewer animals and avoided unnecessary repetition of experiments by simultaneous exploration of all available animal data, thus fulfilling two of the three 3Rs (Reduction and Replacement) (Russell and Burch, 1959).

Improvements for future studies would be, firstly, to include the variability from the LPS stimulation without it interfering with the estimation of the pharmacodynamic effect, for more efficient use of the information provided by the NLME modelling framework. Secondly, although the model has been tested on a large data set with similar characteristics as those found in literature (Chakraborty *et al.*, 2005; Gozzi *et al.*, 1999; Hu *et al.*, 2019; Wang *et al.*, 2007; Wyska, 2010), the model could benefit from being further validated and tested on more TNFα response data. Both to validate that our data analysis well represents the characteristics seen in TNFα response data, and that our proposed framework also works on new data in an even more general setting.

4.2. Contribution to biological meta-analysis

The comparison with previously published work shows that our findings are supported from a biological meta-analysis perspective, and concrete improvements of the modelling framework have been presented. Furthermore, our compilation of published half-lives of TNFα

shows that our estimate of the fractional turnover rate constant k_{out} gives a plausible estimate of TNFα half-life in rodents (8.00 min, Table 3), with the reservation that the published half-lives range from 2.8 min to 82.5 min (Table 6).

To further emphasize the biological relevance, our comparison with previous work (Held *et al.*, 2019) provides a representative overview of what has been achieved with this framework from a meta-analysis perspective (Fig. 8). Starting with LPS (Fig. 8A), we have validated previous findings as well as added inter-occasion variability and a mix of first-order and second-order elimination kinetics to the model. The inclusion of inter-occasion variability led to, amongst others, a new estimate of the IC_{50} of Test Compound A seven times larger than the previous estimate (0.166 μmol/L *versus* 23 nmol/L), highlighting how inter-occasion variability in LPS response can strongly affect drug related parameters if not corrected as done in this work (Held *et al.*, 2019). The mix of first-order and second-order elimination kinetics is based on a finding during the model construction that LPS elimination increased for increasing LPS doses. Three hypotheses for this behaviour are that 1) intravenous injection of endotoxins mimics effects seen in sepsis and rapidly removing LPS from the blood circulation would prevent septic shock (Buttenschoen *et al.*, 2010), 2) the fact that a large amount of LPS is cleared by the liver within ten minutes (Kitchens *et al.*, 2001), and that 3) the size of LPS aggregates influences the uptake of LPS by various tissues (Merck, 2021; Munford *et al.*, 1982) and under the assumption that the percentage of large aggregates should be independent of LPS dose, the amount of large LPS aggregates should increase for increasing doses. However, it is difficult to distinguish between these hypotheses as LPS sensing and signalling is an extensive regulatory network (Buttenschoen *et al.*, 2010; Kitchens *et al.*, 2001; Munford, 2005), and since measurements of LPS are lacking.

Focusing on our contributions to the TNFα meta-analysis (Fig. 8B), we have validated previously found characteristics as well as added new information concerning occasion-dependent peak shifts, flexible handling of different study designs, and multiple *in vivo* test compound interventions. Focusing on multiple *in vivo* test compound interventions, we have shown that the framework can handle positive controls. However, since the maximum inhibition is rapidly reached and persistently kept throughout the duration of the observations for the given oral dose, the pharmacokinetic models for roflumilast and roflumilast N-oxide are technically never used in an exposure dependent (time-varying) way to drive the pharmacodynamics (see Eq. (9)). To improve validation of the model structure allowing for testing of multiple test compounds and comparison of pharmacodynamic effects, the model should be tested on data where the pharmacokinetic model drives the pharmacodynamics in a time-varying way. Nevertheless, although some questions are left unanswered the proposed framework has given good insights in understanding and analysing TNFα response after LPS challenge *in vivo,* both from a mathematical and biological perspective.

5. Conclusions

The goal of this study was to produce a framework of how to model TNFα response in LPS challenge studies *in vivo* and demonstrate its general applicability regardless of occasion or type of test compound. We tested this framework on multiple data sets, in absence or presence of test compounds, and improved our second-generation TNFα turnover model accordingly. From this, accurate model predictions of TNFα response after LPS provocation were retrieved, both on population and individual level, as well as reliable median estimates of the pharmacodynamic effect of both Test Compound A and roflumilast. In addition, the results were compared with previous publications and from a biological perspective determined how we, through our work, could contribute to the meta-analysis concerning LPS challenge studies. Improvements would be to: 1) Implement inter-individual variability from LPS stimulation for TNFα response in presence of test compound, as well as tolerance against LPS, 2) test the framework on more TNFα response data using different LPS doses to further validate the chosen biophase model for LPS and reproducibility of results, and 3) test the framework on TNFα response using other test compounds where the pharmacodynamics are dependent of the pharmacokinetics in a time-varying way.

CRediT Author Statement

Julia Larsson: Methodology, Software, Formal analysis, Investigation, Writing - Original Draft. **Edmund Hoppe:** Conceptualization, Formal Analysis, Resources. **Michael Gautrois:** Formal analysis. **Marija Cvijovic:** Writing - Review & Editing. **Mats Jirstrand:** Conceptualization, Methodology, Writing - Review & Editing, Supervision.

Declaration of Competing Interest

None

Acknowledgements

Julia Larsson was supported by an educational research grant from Grünenthal GmbH. The *in vivo* studies were conducted and monitored by G. Sun, W. Gu, J. Huang, Y. Yang, and L. Xu at Shanghai ChemPartner Co., Ltd. Jacob Leander helped develop expanded functionality to the *NLMEModeling* package for the purpose of this work. This work was also partially funded by the Swedish Foundation for Strategic Research (Grant number AM13-0046).

Supplementary materials

Supplementary material associated with this article can be found, in the online version, at doi:10.1016/j.ejps.2021.105937.

References

Beutler, B.A., Milsark, I.W., Cerami, A., 1985. Cachectin/tumor necrosis factor: production,distribution, and metabolic fate *in vivo*. J Immunol 135 (6), 3972–3977. http://www.jimmunol.org/content/135/6/3972.

Brooks, D., Barr, L.C., Wiscombe, S., McAuley, D.F., Simpson, A.J., Rostron, A.J., 2020. Human lipopolysaccharide models provide mechanistic and therapeutic insights into systemic and pulmonary inflammation. Eur Respir J 56, 1901298. https://doi.org/10.1183/13993003.01298-2019.

Buttenschoen, K., Radermacher, P., Bracht, H., 2010. Endotoxin elimination in sepsis: physiology and therapeutic application. Langenbecks Arch Surg 395 (6), 597–605. https://doi.org/10.1007/s00423-010-0658-6.

Chakraborty, A., Yeung, S., Pyszczynski, N.A., 2005. Pharmacodynamic interactions between recombinant mouse interleukin-10 and prednisolone using a mouse endotoxemia model. J Pharm Sci 94 (3), 590–603. https://doi.org/10.1002/jps.20257.

Dai, C., Fu, Y., Chen, S., Li, B., Yao, B., Liu, W., Zhu, L., Chen, N., Chen, J., Zhang, Q., 2013. Preparation and evaluation of a new releasable PEGylated tumor necrosis factor-alpha (TNF-alpha) conjugate for therapeutic application. Sci China Life Sci 56 (1), 51–58. https://doi.org/10.1007/s11427-012-4431-7.

Earp, J., Krzyzanski, W., Chakraborty, A., Zamacona, M.K., Jusko, W.J., 2004. Assessment of Drug Interactions Relevant to Pharmacodynamic Indirect Response Models. J Pharmacokinet Pharmacodyn 31 (5), 345–380. https://doi.org/10.1007/s10928-004-8319-4.

Gabrielsson, J., Hjorth, S., Vogg, B., Harlfinger, S., Gutierrez, P.M., Peletier, L., Pehrson, R., Davidsson, P., 2015. Modeling and design of challenge tests: Inflammatory and metabolic biomarker study examples. Eur J Pharm Sci 67, 144–159. https://doi.org/10.1016/j.ejps.2014.11.006.

Gottlieb, A.B., Strober, B., Krueger, J.G., Rohane, P., Zeldis, J.B., Hu, C.C., Kipnis, C., 2008. An open-label, single-arm pilot study in patients with severe plaque-type psoriasis treated with an oral anti-inflammatory agent, apremilast. Curr Med Res Opin 24, 1529–1538. https://doi.org/10.1185/030079908X301866.

Gozzi, P., Påhlman, I., Palmér, L., Grönberg, A., Persson, S., 1999. Pharmacokinetic-pharmacodynamic modeling of the immunomodulating agent susalimod and experimentally induced tumor necrosis factor-alpha levels in the mouse. J Pharmacol Exp Ther 291 (1), 199–203.

Hatzelmann, A., Morcillo, E.J., Lungarella, G., Adnot, S., Sanjar, S., Beume, R., Schudt, C., Tenor, H., 2010. The preclinical pharmacology of roflumilast - a selective, oral phosphodiesterase 4 inhibitor in development for chronic obstructive pulmonary disease. Pulm Pharmacol Ther 23 (4), 235–256. https://doi.org/10.1016/j.pupt.2010.03.011.

Held, F., Hoppe, E., Cvijovic, M., Jirstrand, M., Gabrielsson, J., 2019. Challenge model of TNFα turnover at varying LPS and drug provocations. J Pharmacokinet Pharmacodyn 46 (3), 223–240. https://doi.org/10.1007/s10928-019-09622-x.

Holbrook, J., Lara-Reyna, S., Jarosz-Griffiths, H., McDermott, M., 2019. Tumour necrosis factor signalling in health and disease. F1000Res. 8, 111. https://doi.org/10.12688/f1000research.17023.1.

Hu, Y., Wang, L., Xiang, L., Wu, J., Huang, W., Xu, C., Meng, X., 2019. Pharmacokinetic-Pharmacodynamic Modeling for Coptisine Challenge of Inflammation in LPS-Stimulated Rats. Sci Rep 9 (1), 1450. https://doi.org/10.1038/s41598-018-38164-4.

Hurley, J.C., 1995. Endotoxemia: methods of detection and clinical correlates. Clinical microbiology reviews 8 (2), 268–292.

Kitchens, R.L., Thompson, P.A., Viriyakosol, S., O'Keefe, G.E., Munford, R.S., 2001. Plasma CD14 decreases monocyte responses to LPS by transferring cell-bound LPS to plasma lipoproteins. J Clin Invest 108 (3), 485–493. https://doi.org/10.1172/JCI13139.

Kwak, H.J., Song, J.S., Heo, J.Y., Yang, S.D., Nam, J.Y., Cheon, H.G., 2005. Roflumilast inhibits lipopolysaccharide-induced inflammatory mediators via suppression of nuclear factor-kappaB, p38 mitogen-activated protein kinase, and c-Jun NH2-terminal kinase activation. J Pharmacol Exp Ther 315, 1188–1195. https://doi.org/10.1124/jpet.105.092056.

Laporte-Simitsidis, S., Girard, P., Mismetti, P., Chabaud, S., Decousus, H., Boissel, J.-P., 2000. Inter-study variability in population pharmacokinetic meta-analysis: When and how to estimate it? J. Pharm. Sci. 89 (2), 155–167. https://doi.org/10.1002/(SICI)1520-6017(200002)89:2<155::AID-JPS3>3.0.CO;2-2.

Leander, J., Almquist, J., Johnning, A., Larsson, J., Jirstrand, M., 2020. NLMEModeling: A Wolfram Mathematica Package for Nonlinear Mixed Effects Modeling of Dynamical Systems. arXiv preprint. https://arxiv.org/abs/2011.06879.

Li, H., Zuo, J., Tang, W., 2018. Phosphodiesterase-4 Inhibitors for the Treatment of Inflammatory Diseases. Front Pharmacol 9, 1048. https://doi.org/10.3389/fphar.2018.01048.

Lindstrom, M., Bates, D., 1990. Nonlinear mixed effects models for repeated measures data. Biometrics 43, 673–687. https://doi.org/10.2307/2532087.

Lipari, M., Benipal, H., Kale-Pradhan, P., 2013. Roflumilast in the management of chronic obstructive pulmonary disease. Am J Health Syst Pharm 70 (23), 2087–2095. https://doi.org/10.2146/ajhp130114.

Ma, Y., Zhao, S., Shen, S., Fang, S., Ye, Z., Shi, Z., Hong, A., 2015. A novel recombinant slow-release TNF alpha-derived peptide effectively inhibits tumor growth and angiogenesis. Sci Rep 5, 13595. https://doi.org/10.1038/srep13595.

Medzhitov, R., 2008. Origin and physiological roles of inflammation. Nature 454 (7203), 428–435. https://doi.org/10.1038/nature07201.

Merck, 2021. Lipopolysaccharides. https://www.sigmaaldrich.com/technical-documents/protocols/biology/lipopolysaccharides.html (accessed April 16, 2021).

Moritz, T., Niederle, N., Baumann, J., May, D., Kurschel, E., Osieka, R., Kempeni, J., Schlick, E., Schmidt, CG., 1989. Phase I study of recombinant human tumor necrosis factor α in advanced malignant disease. Cancer Immunol Immunothe 29 (2), 144–150.

Munford, R., 2005. Invited review: detoxifying endotoxin: time, place and person. Journal of Endotoxin Research 11 (2), 69–84. https://doi.org/10.1177/09680519050110020201.

Munford, R., Hall, C., Lipton, J., Dietschy, J., 1982. Biological activity, lipoprotein-binding behavior, and in vivo disposition of extracted and native forms of Salmonella typhimurium lipopolysaccharides. The Journal of clinical investigation 70 (4), 877–888.

National Center for Biotechnology Information, 2021. PubChem Compound Summary for CID 449193, Roflumilast. https://pubchem.ncbi.nlm.nih.gov/compound/Roflumilast (accessed April 16, 2021).

Palladino, M., Bahjat, F., Theodorakis, E., Moldawer, L., 2003. Anti-TNF-α therapies: the next generation. Nat Rev Drug Discov 2 (9), 736–746. https://doi.org/10.1038/nrd1175.

Pfalzgraff, A., Weindl, G., 2019. Intracellular Lipopolysaccharide Sensing as a Potential Therapeutic Target for Sepsis. Trends Pharmacol Sci 40, 187–197. https://doi.org/10.1016/j.tips.2019.01.001.

Rojo, Ó.P., Román, A.L.S., Arbizu, E.A., de la Hera Martínez, A., Sevillano, E.R., Martínez, A.A., 2007. Serum lipopolysaccharide-binding protein in endotoxemic patients with inflammatory bowel disease. Inflammatory bowel diseases 13 (3), 269–277. https://doi.org/10.1002/ibd.20019.

Russell W., Burch R, 1959. The principles of humane experimental technique. Methuen & Co. Ltd.

Saks, S., Rosenblum, M., 1992. Recombinant human TNF-alpha: preclinical studies and results from early clinical trials. Immunology series 56, 567–587.

Savic, R., Jonker, D., Kerbusch, T., Karlsson, M., 2007. Implementation of a transit compartment model for describing drug absorption in pharmacokinetic studies. J Pharmacokinet Pharmacodyn 34 (5), 711–726. https://doi.org/10.1007/s10928-007-9066-0.

Schafer, P., 2012. Apremilast mechanism of action and application to psoriasis and psoriatic arthritis. Biochem Pharmacol 83, 1583–1590. https://doi.org/10.1016/j.bcp.2012.01.001.

Scheller, J., Chalaris, A., Garbers, C., Rose-John, S., 2011. ADAM17: a molecular switch to control inflammation and tissue regeneration. Trends Immunol 32 (8), 380–387. https://doi.org/10.1016/j.it.2011.05.005.

Seehase, S., Lauenstein, H.-D., Schlumbohm, C., Switalla, S., Neuhaus, V., Förster, C, Fieguth, H.-G., Pfennig, O., Fuchs, E., Kaup, F.-J., Bleyer, M., Hohlfeld, J.M., Braun, A., Sewald, K, Knauf, S., 2012. LPS-Induced Lung Inflammation in Marmoset Monkeys – An Acute Model for Anti-Inflammatory Drug Testing. Plos One 7, e43709. https://dx.doi.org/10.1371/journal.pone.0043709.

Shibata, H., Yoshioka, Y., Ikemizu, S., Kobayashi, K., Yamamoto, Y., Mukai, Y., Okamoto, T., Taniai, M., Kawamura, M., Abe, Y., Nakagawa, S., Hayakawa, T., Nagata, S., Yamagata, Y., Mayumi, T., Kamada, H., Tsutsumi, Y., 2004. Functionalization of tumor necrosis factor-alpha using phage display technique and PEGylation improves its antitumor therapeutic window. Clin Cancer Res 10 (24), 8293–8300. https://doi.org/10.1158/1078-0432.CCR-04-0770.

Shu, C., Zhou, H., Afsharvand, M., Duan, L., Zhang, H., Noveck, R., Raible, D., 2011. Pharmacokinetic-pharmacodynamic modeling of apratastat: a population-based approach. J Clin Pharmacol 51 (4), 472–481. https://doi.org/10.1177/0091270010372389.

Tisoncik, J., Korth, M., Simmons, C., Farrar, J., Martin, T., Katze, M., 2012. Into the eye of the cytokine storm. Microbiol. Mol. Biol. Rev. 76 (1), 16–32. https://doi.org/10.1128/MMBR.05015-11.

Tsutsumi, Y., Kihira, T., Tsunoda, S., Kamada, H., Nakagawa, S., Kaneda, Y., Kanamori, T., Mayumi, T., 1996. Molecular design of hybrid tumor necrosis factor-alpha III: polyethylene glycol-modified tumor necrosis factor-alpha has markedly enhanced antitumor potency due to longer plasma half-life and higher tumor accumulation. Br J Cancer 74, 1090–1095. https://doi.org/10.1038/bjc.1996.495.

van Eijk, L., John, A., Schwoebel, F., Summo, L., Vauléon, S., Zöllner, S., Laarakkers, C., Kox, M., van der Hoeven, J., Swinkels, D., Riecke, K., Pickkers, P., 2014. Effect of the antihepcidin Spiegelmer lexaptepid on inflammation-induced decrease in serum iron in humans. Blood 124 (17), 2643–2646. https://doi.org/10.1182/blood-2014-03-559484.

van Lier, D., Geven, C., Leijte, G.P., Pickkers, P., 2019. Experimental human endotoxemia as a model of systemic inflammation. Biochimie 159, 99–106. https://doi.org/10.1016/j.biochi.2018.06.014.

Wang, Q., Zhang, Y., Hall, J.P., Lin, L.L., Raut, U., Mollova, N., Green, N., Cuozzo, J., Chesley, S., Xu, X., Levin, J.I., Patel, V.S., 2007. A rat pharmacokinetic/pharmacodynamic model for assessment of lipopolysaccharide-induced tumor necrosis factor-alpha production. J Pharmacol Toxicol Methods 56 (1), 67–71. https://doi.org/10.1016/j.vascn.2007.02.001.

Wyska, E., 2010. Pharmacokinetic-pharmacodynamic modeling of methylxanthine derivatives in mice challenged with high-dose lipopolysaccharide. Pharmacology 85 (5), 264–271. https://doi.org/10.1159/000288734.

Xiang, L., Hu, Y.F., Wu, J.S., Wang, L., Huang, W.G., Xu, C.S., Meng, X.L., Wang, P., 2018. Semi-Mechanism-Based Pharmacodynamic Model for the Anti-Inflammatory Effect of Baicalein in LPS-Stimulated RAW264.7 Macrophages. Front Pharmacol 9, 793. https://doi.org/10.3389/fphar.2018.00793.